Thermochimica Acta 500 (2010) 6–12

Contents lists available at ScienceDirect

Thermochimica Acta

journal homepage: www.elsevier.com/locate/tca

Thermal behaviour of succinic acid, sodium succinate and its compounds with some bivalent transition metal ions

F.J. Caires, L.S. Lima, C.T. Carvalho*, M. Ionashiro

Instituto de Química, Universidade Estadual Paulista, CP 355, 14801-970 Araraquara, SP, Brazil

ARTICLE INFO

Article history:
Received 22 October 2009
Received in revised form
25 November 2009
Accepted 26 November 2009
Available online 29 January 2010

Keywords:
Bivalent transition metals
Succinate
Thermal behaviour

ABSTRACT

Characterization, thermal stability and thermal decomposition of transition metal succinates, $MC_2H_4C_2O_4{\cdot}nH_2O$ (M = Mn(II), Fe(II), Co(II), Ni(II), Cu(II), Zn(II)), the thermal behaviour of succinic acid ($C_4H_6O_4$) and its sodium salt ($Na_2C_2H_4C_2O_4{\cdot}6H_2O$) were investigated employing simultaneous thermogravimetry and differential thermal analysis (TG–DTA), differential scanning calorimetry (DSC), infrared spectroscopy, TG–FTIR system, elemental analysis and complexometry. For the hydrated compounds the dehydration and the thermal decomposition of the anhydrous compounds occur in a single step. For the sodium succinate the final residue up to 545 °C is sodium carbonate, while the transition metal succinates the final residues are Mn_3O_4, Fe_2O_3, Co_3O_4, NiO, CuO and ZnO, respectively. The results also provided information concerning the thermal behaviour and identification of gaseous products evolved during the heating of these compounds.

1. Introduction

The final residues of the thermal decomposition (metal oxides) of metal carboxylates have become a subject of recent interest in view of their diverse applications, such as catalyst, ceramic, dye, photoconductors and so on [1,2]. Furthermore, the succinate anion is very interesting to proposal of crystal engineering due to present various binding modes but also for several conformational modes originating from its flexibility [3].

Although a detailed studies on thermal behaviour of transition metal oxalates have been reported [4,5], a similar study on these metal ions with succinate is lacking. The papers published long ago and only more recent are concerned with the thermal decomposition reactions of metal carboxylate complexes in the solid state [6–8], thermal decomposition reactions of bivalent metal succinates in the solid state [9], the thermal, spectral and magnetic studies of succinic acid compounds of some transitions metal ions [10], precipitation and thermal dehydration of manganese(II) dicarboxylate hydrates [11], synthesis, properties and thermal decomposition of Co(II), Ni(II), Cu(II), Zn(II) and Cd(II) succinates [12], a study of the thermal decomposition of copper(II) and zinc(II) malonate, maleate and succinate complex [13] and a comparative study on the thermal decomposition of some transition metal carboxylates [14]. In all the papers the thermal studies were performed in static atmosphere.

In this paper, the object of the present research was to investigate the thermal behaviour of succinic acid and its sodium salt and to prepare solid-state compounds of some bivalent transition metal ions (i.e. Mn, Fe, Co, Ni, Cu and Zn) with succinate and to characterize and to investigate by means of complexometry, elemental analysis, X-ray powder diffractometry, infrared spectroscopy, simultaneous thermogravimetry and differential thermal analysis (TG–DTA) and differential scanning calorimetry (DSC). The thermal studies were performed in dynamical air atmosphere. The results associated with these compounds are discussed in connection with the papers described in the literature.

2. Experimental

The succinic acid, $C_4H_6O_4$, and the sodium succinate hexahydrated, $Na_2C_2H_4C_2O_4{\cdot}6H_2O$ both with 99% purity were obtained from Sigma.

Carbonates of Mn(II), Fe(II), Co(II), Ni(II), Cu(II) and Zn(II) were prepared by adding slowly with continuous stirring saturated sodium hydrogen carbonate solution to the corresponding metal chloride or sulphate for iron and copper solutions (50.0 mL, 0.15 mol L^{-1}) until total precipitation of the metal ions. The precipitates were washed with distilled water until elimination of chloride or sulphate ions (qualitative test with $AgNO_3/HNO_3$ solution for chloride or $BaCl_2$ solution for sulphate) and maintained in aqueous suspension. To avoid oxidation of Fe(II), all the solutions, as well as the water employed for washing the precipitate were purged with nitrogen gas and the system maintained without contact with air.

* Corresponding author. Tel.: +55 16 3301 6617; fax: +55 16 3322 7932.
E-mail address: ctc.1975@yahoo.com.br (C.T. Carvalho).

0040-6031/$ – see front matter © 2009 Elsevier B.V. All rights reserved.
doi:10.1016/j.tca.2009.11.015

Solid-state Mn(II), Fe(II), Co(II), Ni(II), Cu(II) and Zn(II) compounds were prepared by mixing the corresponding metal carbonates in excess maintained in aqueous suspension with 50.0 mL of succinic acid solution 0.10 mol L^{-1}, and heated slowly up to near ebullition, until total neutralization of the acid. The carbonate in excess was removed by filtration and the aqueous solutions of respective metal succinates were evaporated to near dryness in water bath, dried in air and kept in a desiccator over anhydrous calcium chloride.

In the solid-state compounds, metal ions, hydration water and succinate contents were determined from TG curves. The metal ions were also determined by complexometry with standard EDTA solution after igniting the compounds to the respective oxides and their dissolution in hydrochloric acid solution [15,16].

Carbon and hydrogen contents were determined by microanalytical procedures, with an EA 1110 CHNS-O Elemental Analyser from CE Instruments.

X-ray powder patterns were obtained by using a Siemens D-5000 X-ray diffractometer employing CuKα radiation (λ = 1.541 Å) and settings of 40 kV and 20 mA.

The attenuate total reflectance infrared spectra for sodium succinate and for its metal-ion compounds were run on a Nicolet iS10 FTIR spectrophotometer, using an ATR accessory with Ge window.

Simultaneous TG–DTA and DSC curves were obtained with two thermal analysis system, model SDT 2960 and DSC Q10, both from TA Instruments. The purge gas was an air flow of 100 mL min^{-1} for TG–DTA and 50 mL min^{-1} for DSC experiments. A heating rate of 20 °C min^{-1} was adopted, with sample weighing about 7 mg for TG–DTA and 2 mg for DSC. Alumina and aluminium crucibles, the latter with perforated cover, were used for TG–DTA and DSC, respectively.

The measurements of the gaseous products were carried out using a Thermogravimetric Analyzer Mettler TG–DTA coupled to a FTIR spectrophotometer Nicolet with gas cell and DTGS KBr detector. The furnace and the heated gas cell (250 °C) were coupled through a heated (T = 200 °C) 120 cm stainless steel line transfer with diameter of 2 mm, both purged with dry air (50 mL min^{-1}). The FTIR spectra were recorded with 32 scans per spectrum at a resolution of 4 cm^{-1}.

3. Results and discussion

The TG–DTA curves and IR spectrum of the released product during the heating of succinic acid are shown in Fig. 1. The TG curve, Fig. 1a, shows mass loss in a single step between 165 and 260 °C, and the corresponding DTA curve shows two thermal events. The first and second endothermic peaks at 190 and 250 °C are attributed to the melting and evaporation of succinic acid, respectively and quite different of the thermal behaviour observed for the malonic acid [17]. The succinic acid evaporated was monitored and identified mostly on basis of their FTIR reference available on NICOLET libraries, as shown in Fig. 1b.

For the sodium succinate hexahydrated the TG–DTA curves, Fig. 2, show mass losses in five consecutive and/or overlapping steps and thermal events corresponding to these losses or due to physical phenomenon. The first and second overlapping mass losses between 30 and 150 °C, corresponding to an endotherm with two peaks and 85 and 120 °C are due to dehydration with loss of $6H_2O$ (Calcd. = 40.01%; TG = 39.87%). The anhydrous compound is stable up to 435 °C and the small mass loss (1.1%) observed between 390 and 415 °C is attributed to premature thermal decomposition of the compound provoked by the exothermic peak at 400 °C, probably because the sample temperature surpass momentarily the temperature of thermal decomposition. The last two overlapping steps between 435 and 545 °C, corresponding to the exothermic

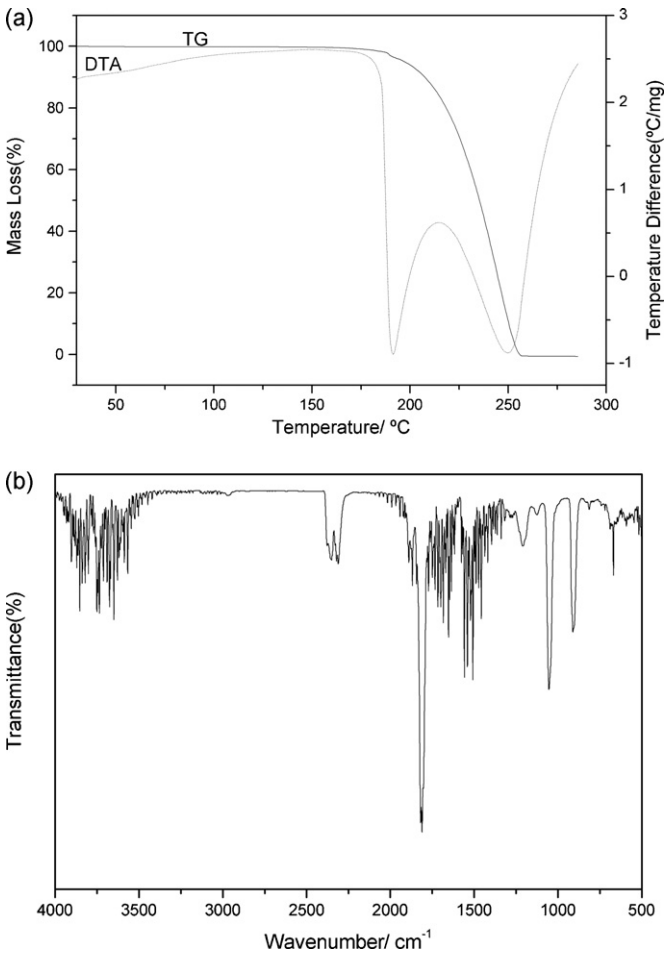

Fig. 1. (a) Simultaneous TG–DTA curves (m = 7.249 mg) and (b) IR spectrum of the gases released during the evaporation of succinic acid.

peaks at 415 and 535 °C are attributed to the oxidation of the products released during the thermal decomposition, with formation of sodium carbonate, as final residue (Calcd. = 39.23%; TG = 39.37%). The exothermic peak at 400 °C followed by an endothermic one at 410 °C is attributed to the solid phase transition and fusion, respectively.

The analytical and thermoanalytical (TG) data for the synthesized compounds are shown in Table 1. These results permitted

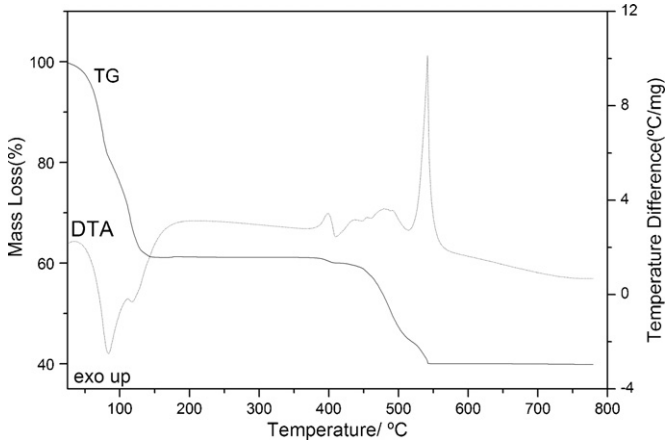

Fig. 2. Simultaneous TG–DTA curves of the sodium succinate hexahydrated (m = 7.234 mg).

Table 1
Analytical data for the $MC_4H_4O_4{\cdot}nH_2O$ compounds.

Compound	Metal oxide (%)			L (lost) (%)		H_2O (%)		C (%)		H (%)		Final residue
	Calcd.	EDTA	TG	Calcd.	TG	Calcd.	TG	Calcd.	E.A.	Calcd.	E.A.	
$MnL{\cdot}2H_2O$	36.84	36.86	36.81	45.75	45.59	17.41	17.60	23.20	23.48	3.90	3.71	Mn_3O_4
$FeL{\cdot}H_2O$	42.04	41.91	41.73	48.47	48.97	9.49	9.30	25.29	25.56	3.19	3.10	Fe_2O_3
$CoL{\cdot}3H_2O$	35.04	34.49	34.94	41.36	41.71	23.60	23.35	20.97	21.15	4.41	4.37	Co_3O_4
$NiL{\cdot}3H_2O$	32.65	32.81	32.30	43.73	43.90	23.62	23.80	20.99	21.07	4.41	4.30	NiO
CuL	44.29	43.94	43.94	55.71	56.06	–	–	26.74	26.51	2.25	2.11	CuO
ZnL	44.84	45.13	44.65	55.16	55.35	–	–	26.48	26.67	2.23	2.35	ZnO

L = succinate.

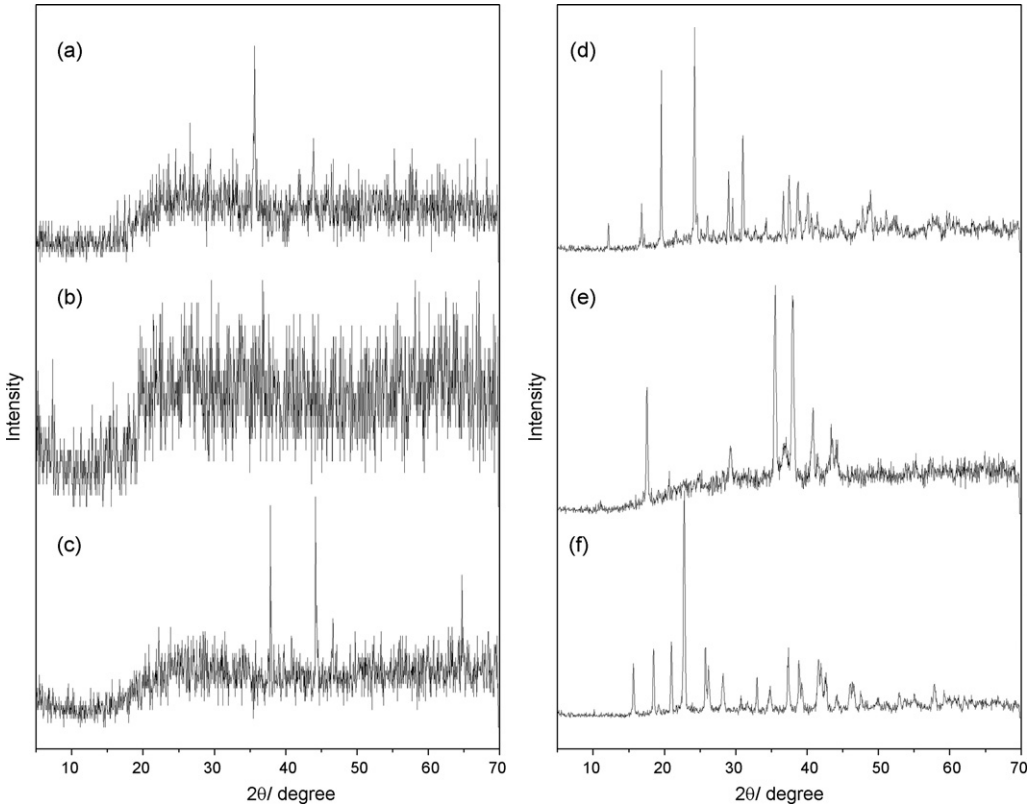

Fig. 3. X-ray powder diffraction patterns of the compounds: (a) $MnL{\cdot}2H_2O$, (b) $FeL{\cdot}H_2O$, (c) $CoL{\cdot}3H_2O$, (d) $NiL{\cdot}3H_2O$, (e) CuL and (f) ZnL (L = succinate).

to establish the stoichiometry of these compounds, which are in agreement with general formula: $MC_4H_4O_4{\cdot}nH_2O$, where M represents Mn(II), Fe(II), Co(II), Ni(II), Cu(II) and Zn(II), $C_4H_4O_4$ is succinate and n = 2(Mn), 1(Fe), 3(Co, Ni) or 0(Cu, Zn).

The X-ray diffraction powder patterns (Fig. 3) showed that the nickel, copper and zinc compounds, have crystalline structure, without evidence for formation of isomorphous ones, while manganese, iron and cobalt compounds were obtained with low crystallinity degree. The difference in the crystallinity of these compounds, must be due to the solubility of each compound and the evaporation velocity which was not controlled, as already observed in the malonate compound with the same transition metal ions [17].

The attenuate total reflectance spectroscopic data on sodium succinate and its compounds with the metal ions considered in this work are shown in Table 2. The investigation was focused mainly within 1700–1400 cm^{-1} range because this region is potentially most informative in attempting to assign coordination sites.

In $Na_2C_4H_4O_4$, strong band at 1536 cm^{-1} and a medium intensity band located at 1402 cm^{-1} are attributed to the anti-symmetrical and symmetrical frequencies of the carboxylate groups, respectively. For the synthesized compounds the anti-symmetrical and symmetrical stretching frequencies are located between 1581–1527 and 1428–1392 cm^{-1}, respectively. Analysis of the frequencies of the ν_{as}(COO) and ν_{sym}(COO) bands indicates that the complexation is carried out through the carboxylate [18] and the infrared spectra data suggest that the bonding of the carboxylate group to the metal is unidentate or pseudo-bridging [19]. This conclusion is supported (at least in the case of the Mn(II), Co(II),

Table 2
Spectroscopic data for sodium succinate and its compounds with some bivalent metal ions.

Compound	ν_{as} (COO^-) cm^{-1}	ν_{sym} (COO^-) cm^{-1}	$\Delta\nu$ ($\nu_{as} - \nu_{sym}$)
$Na_2C_4H_4O_4$	1536 s	1402 m	135
$MnL{\cdot}2H_2O$	1558 s	1410 m	148
$FeL{\cdot}H_2O$	1581 s	1428 m	153
$CoL{\cdot}3H_2O$	1550 s	1404 m	146
$NiL{\cdot}3H_2O$	1536 s	1405 m	131
CuL	1597 s	1430 m	167
ZnL	1527 s	1392 m	135

L = succinate, s = strong, m = medium, ν_{as} (COO^-) and ν_{sym} (COO^-); anti-symmetrical and symmetrical vibrations of the COO^- group, respectively.

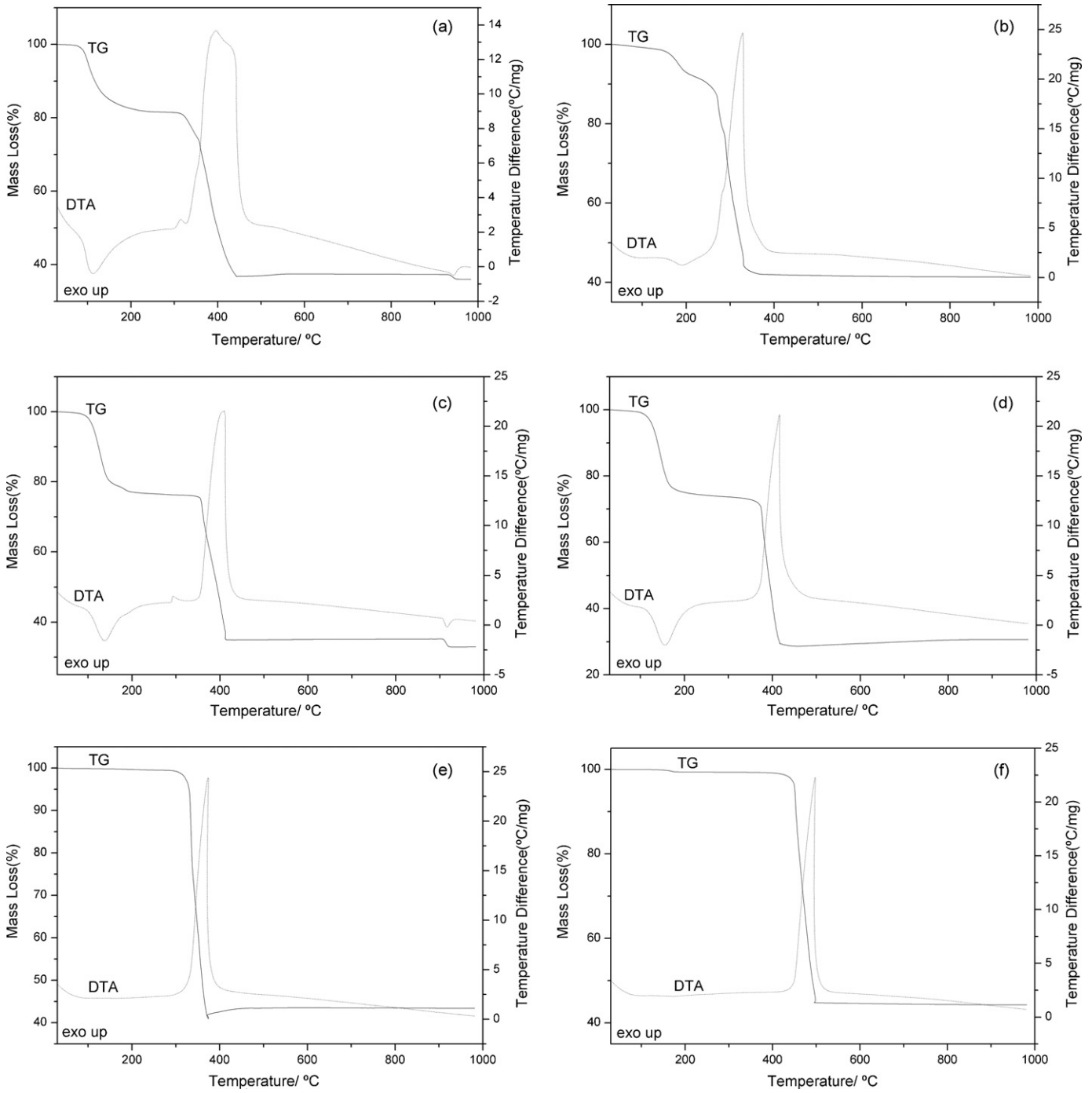

Fig. 4. Simultaneous TG–DTA curves of the compounds: (a) MnL·2H_2O (m = 7.198 mg), (b) FeL·H_2O (7.042 mg), (c) CoL·3H_2O (7.019 mg), (d) NiL·3H_2O (7.105 mg), (e) CuL (7.056 mg) and (f) ZnL (7.085 mg).

Ni(II) and Cu compounds) by the results of the crystal structure determination of manganese(II) succinate tetrahydrate [20–22], tetraaquasuccinato-O,O′-cobalt(II) [23], tetraaquasuccinato-O,O′-nickel(II) [24], succinato-bridged copper(II) complex [25].

Simultaneous TG–DTA and DSC curves of the compounds are shown in Figs. 4 and 5. The TG–DTA curves show mass losses or gain in two or three steps, corresponding to endothermic peak due to dehydration or reduction reaction and exothermic peaks attributed to oxidation of organic matter. The DSC curves also show endothermic and exothermic peaks corresponding to the mass losses displayed by the TG curves. The differences observed concerning the peak temperatures obtained by TG–DTA and DSC curves, even the profiles of the DTA and DSC ones are undoubtedly due to the perforated cover used to obtain the DSC curves, while the TG–DTA ones are obtained without cover, in addition to the experimental conditions which were not the same, too.

The thermal stability of the hydrated (I) or anhydrous compounds (II) and the final temperature of thermal decomposition (III) shown by TG–DTA curves depend on the nature of the metal ion, and they follow the order:

(I) Ni > Mn = Co > Fe;
(II) Zn > Ni > Co > Mn > Cu > Fe;
(III) Zn > Ni = Mn > Co > Fe = Cu.

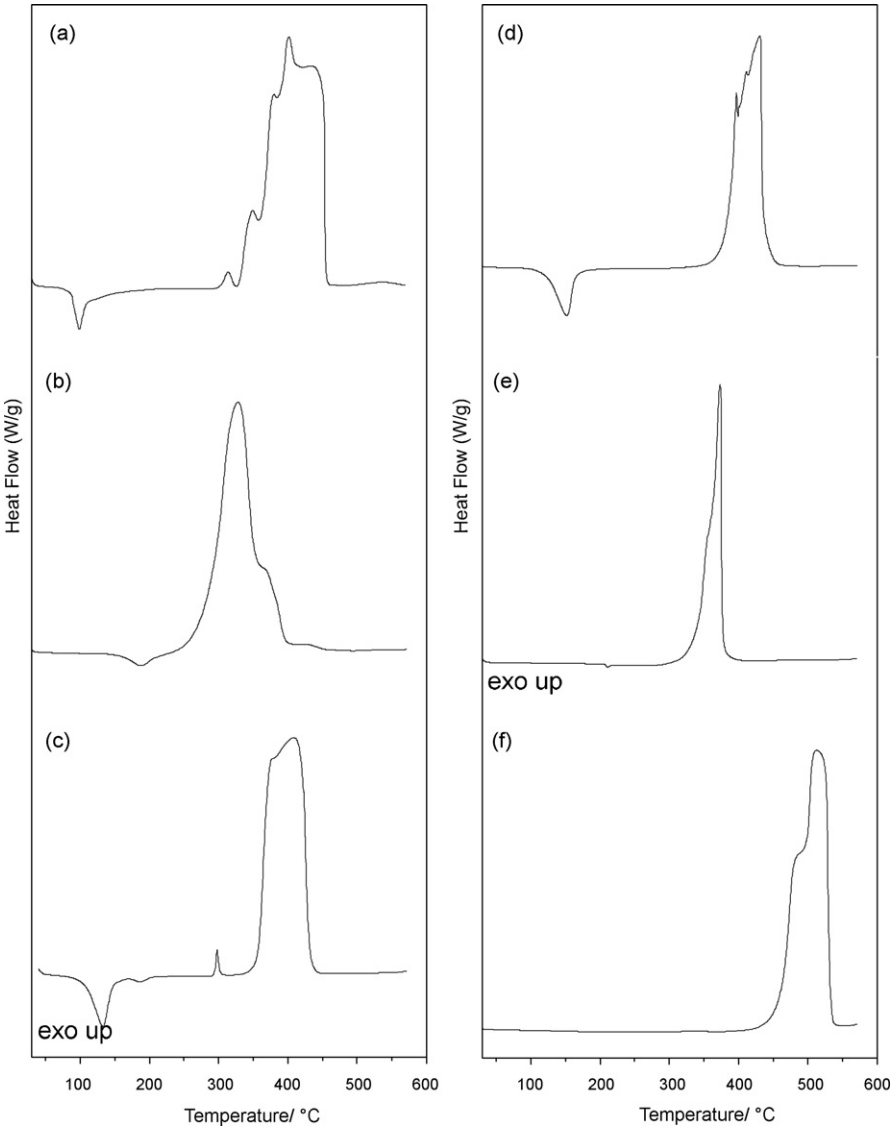

Fig. 5. DSC curves of the compounds: (a) MnL·2H_2O (2.061 mg), (b) FeL·H_2O (2.028 mg), (c) CoL·3H_2O (2.030 mg), (d) NiL·3H_2O (2.000 mg), (e) CuL (1.940 mg) and (f) ZnL (2.088 mg).

The TG–DTA curves also show that the formation of stable anhydrous compounds is observed for manganese, cobalt and nickel ones, while for iron compound the thermal decomposition occurs immediately after the dehydration. The copper and zinc compounds were obtained in the anhydrous state.

The thermal behaviour of the compounds is heavily dependent on the nature of the metal ion and so the features of each of these compounds are discussed individually.

3.1. Manganese compound

The simultaneous TG–DTA and DSC curves are shown in Figs. 4a and 5a, respectively. The first mass loss observed between 70 and 180 °C (TG), corresponding to an endothermic peak at 110 °C (DTA) and 99 °C (DSC) is due to dehydration with loss of 2H_2O (Calcd. = 17.41%, TG = 17.60%). The thermal decomposition of the anhydrous compounds occurs in a single step, between 315 and 415 °C with loss of 45.59%, corresponding to the exothermic peak at 400 °C (DTA) or an exotherm with peaks at 402 and 436 °C (DSC), which are attributed to the oxidation of the organic matter. The total mass loss up to 400 °C is in agreement with the formation of Mn_3O_4 (Calcd. = 63.16%, TG = 63.19%). The last mass loss observed between 930 and 960 °C corresponding to an endothermic peak at 945 °C is assigned to the reduction of Mn_3O_4 to MnO in agreement with the literature [26]. The small exothermic peak at 315 °C (DTA) or 314 °C (DSC) is due to the recrystallization process, as can be seen in Fig. 6.

3.2. Iron compound

The simultaneous TG–DTA and DSC curves are shown in Figs. 4b and 5b, respectively. The first mass loss observed between 50 and 210 °C (TG), corresponding to endothermic peak at 195 °C (DTA) or 188 °C (DSC) is due to dehydration with loss of 1H_2O (Calcd. = 9.49%, TG = 9.30%). Immediately after the dehydration, the anhydrous compound shows mass loss in a single step between 210 and 375 °C with loss of 48.97%, corresponding to the exothermic peak at 325 °C (DTA) and 328 °C with shoulder at 364 °C (DSC), attributed to the oxidation of Fe(II) to Fe(III) and organic matter. The total mass loss up to 375 °C is in agreement with the formation of Fe_2O_3, as final residue (Calcd. = 57.96%, TG = 58.27%), which was confirmed by X-ray powder diffractometry.

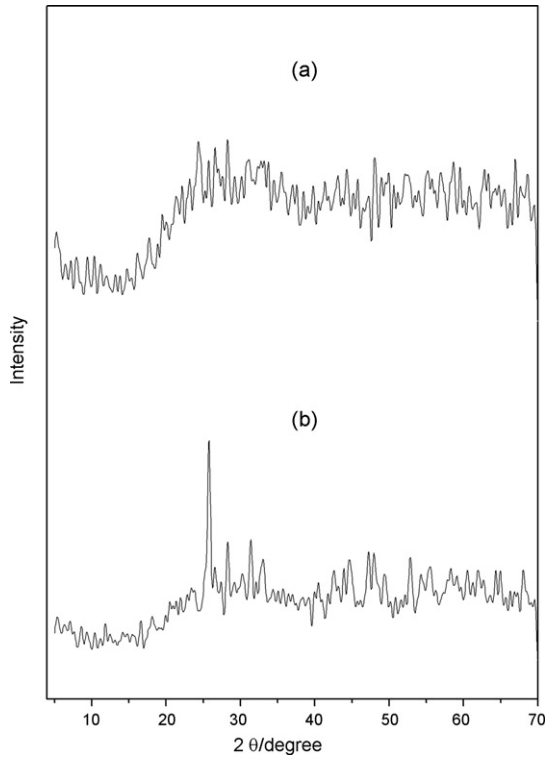

Fig. 6. X-ray powder diffraction patterns: (a) heated up to 200 °C and (b) heated up to 325 °C.

3.3. Cobalt compound

The simultaneous TG–DTA and DSC curves are shown in Figs. 4c and 5c, respectively. The first mass loss that occurs between 70 and 195 °C (TG), corresponding to endothermic peak at 140 °C (DTA) or 134 °C (DSC) is due to dehydration with loss of $3H_2O$ (Calcd. = 23.60%, TG = 23.35%). The thermal decomposition of the anhydrous compound occurs in a single step between 345 and 420 °C with loss of 41.71%, corresponding to exothermic peak at 410 °C (DTA) or 408 °C with shoulder at 377 °C (DSC), attributed to oxidation of the organic matter. The total mass loss up to 410 °C is in agreement with the formation of Co_3O_4 (Calcd. = 64.96%, TG = 65.06%). The last mass loss that occurs between 905 and 925 °C, corresponding to the endothermic peak at 915 °C (DTA) is attributed to reduction of Co_3O_4 to CoO (Calcd. = 2.33%, TG = 2.13%) in agreement with the literature [27,28]. The X-ray powder pattern of the residue obtained at 950 °C is coincident with that one obtained for Co_3O_4; this is due to the oxidation reaction of CoO to Co_3O_4, which occurs on cooling the former in an air atmosphere at room temperature [28]. The exothermic peak at 295 °C (DTA) or 299 °C (DSC) without mass loss in the TG curve is due to the solid phase transition, since no recrystallization process was observed in the X-ray powder pattern with samples heated after and before the exothermic peak.

3.4. Nickel compound

The simultaneous TG–DTA and DSC curves are shown in Figs. 4d and 5d, respectively. The mass loss that occurs between 85 and 185 °C, corresponding to endothermic peak at 155 °C (DTA) or 152 °C (DSC), is due to dehydration with loss of $3H_2O$ (Calcd. = 23.62%, TG = 23.80%). After the dehydration the thermal decomposition occurs in a single step between 350 and 450 °C with loss of 43.80%. This mass loss corresponding to the exothermic peak

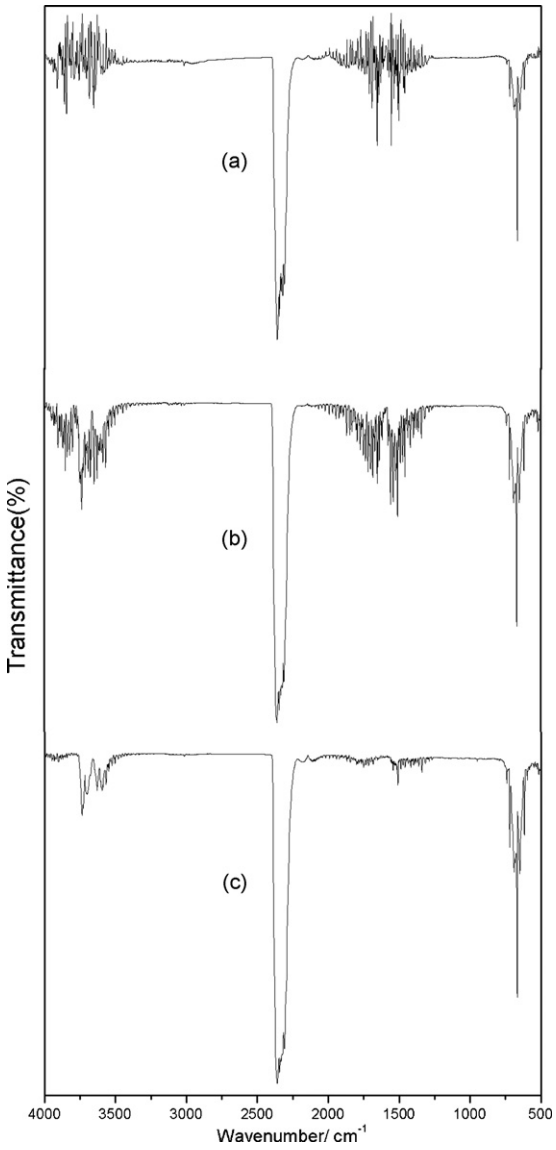

Fig. 7. IR spectra of gaseous products evolved during the decomposition of the compounds: (a) NaL·$6H_2O$, (b) NiL·$3H_2O$, and (c) ZnL (L = succinate).

at 420 °C (DTA) or an exotherm with peaks at 397, 412 and 431 °C (DSC) is attributed to oxidation of the organic matter. The total mass loss up to 450 °C is in agreement with the formation of NiO, as final residue (Calcd. = 67.35%, TG = 67.70%) and confirmed by X-ray powder diffractometry.

3.5. Copper compound

The simultaneous TG–DTA and DSC curves are shown in Figs. 4e and 5e, respectively. These curves show that the compound is anhydrous and stable up to 300 °C. Above this temperature the thermal decomposition occurs in a single step between 300 and 375 °C with loss of 56.06% corresponding to the exothermic peak at 375 °C (DTA) or 373 °C (DSC) attributed to oxidation of organic matter. The mass loss up to 375 °C is in agreement with the formation of the Cu_2O as residue (Calcd. = 60.17%, TG = 59.03%). The mass gain that occurs between 375 and 530 °C, is attributed to the oxidation of Cu(I) to Cu(II) with formation of CuO as final residue (Calcd. = 55.71%, TG = 56.06%), which was confirmed by X-ray powder diffractometry.

3.6. Zinc compound

The TG–DTA and DSC curves are shown in Figs. 4f and 5f, respectively. These curves also show that the compound was obtained in the anhydrous state and stable up to 405 °C. Above this temperature the thermal decomposition occurs between 405 and 500 °C with loss of 55.35%, corresponding to the exothermic peak at 495 °C (DTA) or 513 °C with shoulder at 486 °C (DSC) attributed to oxidation of organic matter. The total mass loss up to 500 °C is in agreement with the formation of ZnO, as final residue (Calcd. = 55.16%, TG = 55.35%), which was confirmed by X-ray powder diffractometry.

The thermal stability, temperature range of mass loss and the TG–DTA profiles are in disagreement with the data reported by Allan and Carson [10]. The disagreement is also observed in the dehydration temperature and thermal stability of the anhydrous compounds, as well as the thermal decomposition residue, reported by Randhawa and Gandotra [14]. These disagreements undoubtedly are due to the static air atmosphere used to obtain the TG and DTA curves in the work of Refs. [10,14], while, in the present paper dynamic air atmosphere was used for the TG and DTA ones. It is well known that the experimental conditions affect the TG and DTA curves. For the dynamic atmosphere the evolved products of the thermal decomposition are continuously changed while in the static atmosphere the same is not observed. On that account the disagreements are observed.

The gaseous products evolved during the thermal decomposition of the sodium and transition metal ion compounds studied in this work were monitored by FTIR, and it has carbon dioxide as main product due to the decarboxylation and oxidation of organic matter. The IR spectra of the gaseous products evolved during the thermal decomposition of sodium, cobalt and zinc succinates, as representative of all the compounds are shown in Fig. 7.

4. Conclusion

From TG, complexometry and elemental analysis data, a general formula could be established for the binary compounds involving some bivalent metal ions and $C_4H_4O_4$. The X-ray powder patterns pointed out that the nickel, copper and zinc the compounds have a crystalline structure without evidence concerning the formation of isomorphous compounds, while manganese, iron and cobalt ones showed low crystallinity degree.

The infrared spectroscopic data suggests that $C_4H_4O_4$ acts as a unidentate or pseudo-bridging ligand towards the metal ions considered in this work.

The TG–DTA and DSC curves provided previously unreported information about the thermal stability and thermal decomposition of these compounds in dynamic air atmosphere.

The monitoring of evolved gases during the heating of succinic acid showed that the acid evaporate without decomposition. The thermal decomposition of metal succinates occurs preferentially with the release of carbon dioxide due to decarboxylation and oxidation of organic matter.

Acknowledgements

The authors thank FAPESP, CNPq and CAPES Foundations for financial support.

References

[1] A.S. Malik, M.J. Duncan, P.G. Bruce, J. Mater. Chem. 13 (2003) 2123–2126.
[2] V.E. Henrich, P.A. Cox, The Surface Science of Metal Oxides, Combridge University Press, 1994.
[3] D. Ghoshal, T.K. Maji, G. Mostafa, S. Sain, T.-H. Lu, J. Ribas, E. Zangrando, N. Ray Chaudhuri, Dalton Trans. (2004) 1687–1695.
[4] D. Dollimore, D.L. Griffiths, J. Therm. Anal. 2 (1970) 229–250.
[5] M.A. Mohamed, A.K. Galwey, S.A. Halawy, Thermochim. Acta 429 (2005) 57–72.
[6] H.L. Saha, S. Mitra, Thermochim. Acta 109 (1987) 331–342.
[7] H.L. Saha, S. Mitra, Thermochim. Acta 112 (1987) 275–287.
[8] H.L. Saha, S. Mitra, Thermochim. Acta 116 (1987) 53–64.
[9] H. Yokobayashi, K. Nagase, K. Muraishi, Bull. Chem. Soc. Jpn. 48 (1975) 2789–2792.
[10] J.R. Allan, B.R. Carson, Thermochim. Acta 158 (1990) 91–97.
[11] Y. Suzuki, Thermochim. Acta 255 (1995) 155–170.
[12] W. Brzyska, B. Galkowska, Polish J. Chem. 72 (1998) 498–503.
[13] A.K. Nikumbh, S.K. Pardeshi, M.N. Raste, Thermochim. Acta 374 (2001) 115–128.
[14] B.S. Randhawa, K. Gandotra, J. Therm. Anal. Calorim. 85 (2006) 417–424.
[15] H.A. Flaschka, EDTA Titrations, Pergamon Press, Oxford, 1964.
[16] C.N. de Oliveira, M. Ionashiro, C.A.F. Graner, Ecl. Quim. 10 (1985) 7–10.
[17] F.J. Caires, L.S. Lima, C.T. Carvalho, R.J. Giagio, M. Ionashiro, Thermochim. Acta, in press.
[18] K. Nakamoto, Infrared and Raman Spectra of Inorganic and Coordination Compounds Part B, 5th ed., Wiley, New York, 1997, pp. 58–61.
[19] G.B. Deacon, R.J. Phillips, Coord. Chem. Rev. 33 (1980) 227–250.
[20] M.P. Gupta, R.D. Sahu, R. Ram, P.R. Maulik, Z. Kristallogr. 163 (1983) 155–158.
[21] M. Fleck, E. Tillmans, L. Bohaty, Z. Kristallogr. 215 (2000) 429–430.
[22] Y.-Q. Zheng, J. Sun, J.-L. Lin, Z. Kristallogr. 217 (2002) 411–412.
[23] Y.-Q. Zheng, J.-L. Lin, Z. Kristallogr. 215 (1) (2000) 159–160.
[24] Y.-Q. Zheng, J.-L. Lin, Z. Kristallogr. 215 (1) (2000) 157–158.
[25] D. Ghoshal, A.K. Ghosh, G. Mostafa, J. Ribas, N.R. Chaudhuri, Inorg. Chim. Acta 360 (2007) 1771–1775.
[26] L. Biernacki, S. Pokrzywnicki, J. Therm. Anal. Calorim. 55 (1999) 227–232.
[27] G.A. El-Shobaky, A.S. Ahmad, A.N. Al Noaim, H.G. El-Shobaky, J. Therm. Anal. 46 (1996) 1801–1808.
[28] Z.P. Xu, H.C. Zeng, J. Mater. Chem. 8 (11) (1998) 2499–2506.